PORTLAND METAKAOLIN CEMENT CONTAINING DOLOMITE OR LIMESTONE – SIMILARITIES AND DIFFERENCES IN PHASE ASSEMBLAGE AND COMPRESSIVE STRENGTH

Alisa Machner[1,3,*], Maciej Zajac[2], Mohsen Ben Haha[2], Knut O. Kjellsen[3], Mette R. Geiker[1], Klaartje De Weerdt[1]

[1]NTNU Department of Structural Engineering, Richard Birkelandsvei 1A, 7034 Trondheim, Norway
[2]Heidelberg Technology Center GmbH, Oberklammweg 2-4, 69181 Leimen, Germany
[3]Norcem AS, R&D Department, Setreveien 2, 3991 Brevik, Norway

*Corresponding author: alisa.machner@ntnu.no
+47 45394622
ORCID-ID: 0000-0002-6334-5116

ABSTRACT

The scarceness of high-quality limestone obliges the cement industry to consider alternative supplementary cementitious materials (SCMs) for the production of blended cements. This study investigated the potential usage of dolomite instead of limestone as an addition to Portland metakaolin cement by measuring the development of the compressive strength and phase assemblages at 5 °C, 20 °C or 38 °C. Laboratory grade materials were used to identify potential differences in the impact of the carbonate on the phase assemblages. As with limestone, a strength increase was observed when dolomite is added at temperatures >5 °C due to the formation of additional carbonate AFm phases and the stabilization of ettringite. Differences were observed in the amount and type of the carbonate AFm and AFt phases formed. Thermodynamic modelling in combination with the experimental results indicate that the dolomite and limestone affect Portland metakaolin cement in a similar way, with the reactivity being the major difference between the two carbonate sources. This indicates that with regard to the strength development up to 90 days dolomite can be used instead of limestone to replace parts of a Portland metakaolin cement.

Keywords: curing temperature; blended cements; ettringite stabilization; rate of reaction; thermodynamic modelling

INTRODUCTION

There are several ways to minimize the effect of cement production on our climate, one of which is to use supplementary cementitious materials (SCMs) [1]. Limestone is widely used as an SCM. According to the European standard EN197-1, it can replace up to 5%wt clinker in CEM I Portland cements and up to 35%wt in CEM II Portland-limestone cements [2].

The addition of finely ground limestone to Portland cement affects the hydration in two ways. First, there is the physical effect of finely ground limestone, which is also often called the filler effect. The addition of fine materials to Portland cement provides additional nucleation sites, which facilitate the formation of hydrates during the hydration of the cement. Moreover, in systems where parts of the cement are replaced by another material, the water-to-cement ratio increases when the water-to-solid ratio is kept constant. This increases the reaction degree of the cement. The addition of finely-ground limestone is known to enhance the reaction of alite and therefore of Portland cement [3,4], and can also shorten the time necessary to nucleate the first C-S-H phase [5], which accelerates the hydration of the cement. However, the filler effect is also always connected with a dilution effect, because the most reactive part of the system is replaced with a less-reactive material.

Second, and contrary to earlier understanding that limestone is an inert material, several authors have reported a reaction of limestone when added to Portland cement [6,7]. Carbonate AFm phases, such as hemicarbonate and monocarbonate, are formed during the reaction of limestone with pure C_3A or C_3A in Portland cement [8–12]. In the presence of carbonates, these AFm phases are more stable than monosulphate [13]. Consequently, the ettringite does not transform to monosulphate after the sulphate source, e.g. gypsum, is depleted. This chemical effect is called ettringite stabilization and results in a relative increase in the volume of hydrates and leads to an increase in compressive strength at low replacement levels [6,7]. A comprehensive overview of

58 the effect of limestone addition to Portland cement on compressive strength and phase
59 assemblage can be found in [14].
60
61 The high-grade limestone required by EN197-1 [2] is not sufficiently available in all parts of the
62 world, so various other carbonate sources are in the focus of ongoing research, with dolomite rock
63 being one promising alternative. Schöne et al. [15] observed similar compressive strength results
64 from cements where 23%wt was replaced with either limestone or dolomite. Moreover, Zajac et
65 al. were able to demonstrate that the effect of ettringite stabilization upon carbonate addition,
66 which has been known for cements containing limestone, is also valid for cements containing
67 ground dolomite rock [16].
68
69 The mineral dolomite, which is petrogenetic for dolomite rock, is not stable in the high-alkaline
70 environment of a cement and has been reported to undergo what is known as the
71 dedolomitization reaction [17,18]. In this reaction, dolomite reacts with calcium hydroxide
72 (portlandite) to form calcium carbonate (calcite) and magnesium hydroxide (brucite). However,
73 it has been shown that, in cementitious systems where other ions (Al, Si) are present, the reaction
74 of dolomite produces products similar to those of hydrating Portland limestone cement and
75 hydrotalcite [16,19].
76
77 The dissolution of dolomite and calcite in various conditions has been studied before [20].
78 Pokrovsky et al. were able to show that the dissolution rate of dolomite is significantly smaller
79 than that of limestone at both 25 °C and 60 °C [21]. Moreover, the dissolution rates of both
80 decrease with increasing pH [22] and increase with increasing temperatures from 25 °C to 60 °C
81 [21]. This accords with other authors, who have reported a higher degree of reaction of dolomite
82 with increasing temperatures [19,23].
83

The positive effect of adding carbonate to ordinary Portland cements is limited because the amount of alumina available is limited in these cements. However, the effect can be amplified by increasing the aluminium content of the cement by using various aluminium-containing SCMs. This synergetic effect has previously been demonstrated for samples containing limestone and fly ash [24,25] and for combinations of limestone and metakaolin [26–28].

In the present study, we used a calcined clay-containing Portland composite cement with a cement-to-metakaolin ratio of 6:1 to ensure an aluminium-rich cement, referred to in the following as Portland metakaolin cement (CM). We investigated the phase assemblage development of this Portland metakaolin cement with various levels of carbonate addition, either pure dolomite or limestone, in pastes over hydration periods of up to 90 days. We also measured the compressive strength of mortar samples with the same compositions. To investigate the effect of curing at different temperatures, samples were cured at 5 °C and 38 °C as well as the usual 20 °C.

EXPERIMENTAL

MATERIALS

The materials used for this study were Portland cement clinker (C, from Norcem), and laboratory-grade dolomite (D, Magnesia 4179 from Brenntag), limestone (L, Magnesia 4491 from Brenntag) metakaolin (M, Metastar501 from Imerys) and gypsum ($, $CaSO_4 \cdot 2H_2O$, from Merck). The cement clinker was ground in a laboratory ball mill until a Blaine surface area of approx. 400 m^2/kg was achieved. The other materials were used as received. All materials were characterized by means of XRF (Table 1), QXRD (Table 2, Table 3), Blaine specific surface area (Table 1), and laser diffraction (Figure 1). Laboratory-grade materials were used to make it possible to investigate the effect of dolomite without calcite impurities. The dolomite used was synthesized by precipitation, which is why it has a much finer particle size distribution than the limestone used.

The experimental matrix is given in Table 4. The reference 100CM represents a model composite cement consisting of Portland cement clinker and metakaolin with the mass ratio of 6:1. Levels of 5, 10 or 20%wt of the composite cement were replaced by either limestone or dolomite. To ensure a sufficient sulphate content in the samples, 2.85%wt of laboratory-grade gypsum was added to all mixes.

The paste samples were prepared in the laboratory at 20 °C by mixing binder and water with a w/b ratio = 0.55 (due to the high fineness of the materials used) in a Braun MR5550CA high shear mixer. The mixing procedure was: mixing for 30 s, resting for 5 min, and mixing again for 60 s. The pastes were then cast in 12 ml plastic tubes (diameter 23 mm), which were sealed and stored at the various temperatures over water for up to 90 days.

The mortar samples were prepared in accordance with EN 196-1 [29], except that the w/b ratio had to be increased to 0.55 due to the high fineness of the materials used. After 1 day in a climate chamber (20 °C, >90% RH) the prisms (40x40x160 mm) were demoulded and stored in big tanks immersed in lime water together with other samples at 20 °C until measurement. Additional samples for the other temperatures (5 °C and 38 °C) were prepared in a similar way, except that they were not stored in a climate chamber for the first day, but in their moulds in a closed box over water at their respective temperatures. After 1 day, they were demoulded and stored immersed in lime water at their respective curing temperatures. The samples cured at 38 °C were stored in 20-litre plastic boxes filled with lime water and not in the big tanks as the other samples. The mortar and paste samples were investigated after 1, 28 and 90 days of hydration at 20 °C. The samples cured at 5 °C and 38 °C were investigated after 28 and 90 days.

METHODS

DOUBLE SOLVENT EXCHANGE

After 1 day (only for samples stored at 20 °C), 28 days, and 90 days, the hydration was stopped by means of double solvent exchange. First, a 6 mm thick slice (diameter: 23 mm) was cut off the cured cement paste sample. The paste was crushed in a porcelain mortar until the whole sample had passed through a 1 mm sieve. The coarsely crushed cement paste was then immersed in 50 ml isopropanol, shaken for 30 seconds, and left to rest for 5 min before the isopropanol was poured off. This isopropanol treatment was performed twice before the sample was transferred to a filtration unit where the isopropanol was filtrated out and the paste was immersed in 10 ml petroleum ether. After 30 seconds of stirring, the suspension was left to rest for 5 minutes. The sample was then vacuum-filtrated and subsequently dried overnight in a desiccator under a slight vacuum (-0.2 bar) applied using a water pump. All the samples were stored in a desiccator over silica gel and soda lime until measurement. The grinding of the samples to fine powder (< 63 µm) was generally performed on the day of measurement.

TGA

Thermogravimetric analysis (TGA) was performed on all the pastes after the double solvent exchange treatment, drying and grinding. For the TGA measurements, the powders were poured into 600 µl corundum crucibles and stored in a sample changer until measurement (max. 8 h). The weight loss was measured from 40–900 °C with a heating rate of 10 °C/min in a Mettler Toledo TGA/DSC3+ device. During the measurement, the measurement cell was purged with 50 ml/min of nitrogen gas. TGA was used to quantify the mass loss due to the loss of bound water (H) and the decomposition of portlandite (CH). The weight loss of the portlandite between approx. 400 °C and 550 °C was determined with a tangential step. The bound water was determined by the difference between the sample weight at 50 °C and approx. 550 °C using a horizontal step. The sample weight at approx. 550 °C was assumed to be the dry binder weight, which would remain constant during the cement hydration. At higher temperatures, the carbonates present in the composite cements

would decompose and cause additional mass loss. The equations for the quantification of bound water (H) and portlandite (CH) relative to the dry mass or clinker content (c.f. [30]) are given in Eq. 1–4:

$$H_{dry} = \frac{w_{50} - w_{550}}{w_{550}} \quad (1)$$

$$CH_{dry} = \frac{w_{400} - w_{550}}{w_{550}} \; x \; \frac{74}{18} \quad (2)$$

$$H_{clinker} = \frac{w_{50} - w_{550}}{w_{550}} \; x \; \frac{100}{\%\, clinker} \quad (3)$$

$$CH_{clinker} = \frac{w_{400} - w_{550}}{w_{550}} \; x \; \frac{74}{18} \; x \; \frac{100}{\%\, clinker} \quad (4)$$

The standard deviations of these quantifications were calculated based on three independent measurements of the 100CM sample. For the portlandite quantification, the standard deviation was 0.8%wt and for the bound water content 1.2%wt. This is illustrated as error bars in the figures.

XRD

X-ray diffraction (XRD) analyses were performed on the same pastes as those used for TGA. For the XRD analyses, the powder was loaded into the sample holders by means of front loading and queued in a sample changer until measurement (max. 5 h). A D8 Focus diffractometer from Bruker was used for the measurements with a Bragg-Brentano θ–2θ geometry and a goniometer radius of 200.5 mm. The samples were measured between 5 °2θ and 55 °2θ with a step size of 0.01 °2θ and a sampling time per step of 0.5 s. Cu-Kα radiation with a wavelength of approx. 1.54 Å was used as the X-ray source. The divergence slit was fixed at 0.2 mm and the Soller slits were set to 2.5°. The XRD plots were qualitatively evaluated using DIFFRAC.EVA V4.0 software from Bruker. All observations regarding peak height and shape are only used as an indication, and is used together with the TGA results.

MERCURY INTRUSION POROSIMETRY

To make it possible to study the threshold pore diameter and total porosity of the paste samples with mercury intrusion porosimetry (MIP), a 7 mm slice of the cured cement paste was cut off each sample and coarsely crushed in a porcelain mortar. The crushed samples were then immersed in isopropanol for at least 24 h and then dried in an aerated oven overnight at 40 °C to remove the isopropanol. A Pascal 140/440 porosimeter from Thermo Scientific was used to get the MIP measurements. The first intrusion curve reported from the measurements was used to determine the threshold pore diameter and the pore volume, which equals the total porosity measurable with MIP.

COMPRESSIVE STRENGTH TESTING

After 1, 28 and 90 days of hydration, the compressive strength of the mortar prisms was determined in accordance with EN 196-1 [29]. For every testing time, two mortar prisms were split in two and the compressive strength of all four resulting specimens was measured. The average and standard deviations of all four results were calculated and plotted in the figures.

THERMODYNAMIC MODELLING

The Gibbs free energy minimization program GEMS [31,32] was used to model how the hydrate phase assemblages and their volumes depend on the degree of reaction of either dolomite or limestone. The thermodynamic data used from the PSI-GEMS database was supplemented with a cement specific database (CEMDATA14 database) [33–35], which includes solubility products of the solids relevant for cementitious materials. For the C-S-H phase, the CSHQ model proposed by Kulik was used [36]. In the case of hydrogarnets, the solid solution model for Al-Fe siliceous hydrogarnets was used [37]. The effect of the degree of reaction of dolomite or limestone on phase assemblage was investigated. The samples 95CM5D and 95CM5L were used for the geochemical modelling at 20 °C. The composition of the Portland metakaolin cement used as an input for the

model was calculated from the XRF results given in Table 1. In this work, we used the same modelling approach as in [38]. However, we assumed the constant hydration degree of clinker and metakaolin to be 100%.

RESULTS & GENERAL DISCUSSION

COMPRESSIVE STRENGTH

Figure 2 a-c shows the development of the compressive strength of the various compositions investigated for the various curing times and curing temperatures tested.

After 1 day of curing at 20 °C, increasing replacement of CM by either of the carbonates led to slightly decreasing compressive strengths (Figure 2 b). Moreover, there were no notable differences between the samples containing limestone and dolomite. This indicates that any strength increase observed for minor carbonate replacements after 28 or 90 days of curing cannot be caused only by physical filler effects because this should already be visible after 1 day of curing.

Figure 2 b shows that, after 28 and 90 days of curing at 20 °C, the compressive strength increased compared to the 100CM mortar with limestone additions of up to 5%wt and with dolomite additions of up to 10%wt, and decreased again at higher replacement levels. For the 28d and 90d samples at 20 °C, the highest overall compressive strength was shown by the 95CM5L sample. It should be noted that at a replacement level of 20%wt the 80CM20D sample showed slightly higher compressive strength than the 80CM20L sample when cured at 20 °C.

The development of the compressive strength changed at the other curing temperatures. At 5 °C (Figure 2a), the positive effect of limestone addition on compressive strength could be observed for a replacement level of 5%wt. At higher replacement levels, the compressive strength values decreased. The replacement of CM by dolomite resulted in the reduction of the compressive strength at all replacement levels. Moreover, for replacement levels < 20%wt, all the samples

containing limestone showed higher compressive strength values than the samples containing dolomite. The positive effect of carbonate addition on compressive strength was generally less pronounced and the total compressive strength values were lower for samples cured at 5 °C than for the samples cured at 20 °C.

Figure 2c shows that, after 28 and 90 days of curing at 38 °C, the compressive strength levels were similar or even lower for samples containing limestone than for samples containing dolomite. At 38 °C, the positive effect of carbonate addition on the compressive strength was only visible for the samples containing dolomite. The samples containing limestone showed no increased compressive strength for any replacement level. However, we can not report on a possible increase in compressive strength at lower replacement levels than 5%wt. It should be noted, that the differences between samples containing limestone and dolomite were relatively small at 38 °C compared to the differences observed at lower temperatures. The highest compressive strength values were achieved in samples containing 5%wt of dolomite.

MERCURY INTRUSION POROSIMETRY

Figure 3 a-c shows the development of the threshold diameter and the porosity for the various replacement levels of either dolomite or limestone at the various curing temperatures after 90 days of hydration.

The results for the samples containing dolomite and limestone are generally very similar. Differences in the particle size distribution of the two carbonate sources seem to have no significant influence on the microstructure of the paste samples.

At 5 °C, the porosity of the samples increased for all replacement levels of dolomite compared to the CM sample. The sample containing 5%wt limestone showed a slightly decreased porosity. At higher replacement levels than 5%wt of limestone, the porosity increased again. The threshold

pore diameter decreased for all replacement levels of either dolomite or limestone. The samples containing limestone showed a higher threshold diameter for the 20%wt replacement level than the samples containing dolomite. The reason for this is unclear.

At 20 °C, the trends with increasing replacement levels of either dolomite or limestone are very similar. In both cases, the addition of 5%wt of a carbonate source reduced the porosity slightly. At higher replacement levels, the porosity increased. The threshold diameter increased with every replacement level from 5%wt and upwards compared to the CM sample.

At 38 °C, the results for the threshold diameter are similar to the samples cured at 20 °C, but the porosity of the samples was slightly higher. Moreover, at a replacement level of 5%wt, the porosity decreased for the 95CM5D sample but stayed almost constant for the 95CM5L sample. At higher replacement levels, the porosity of the samples containing dolomite increased. The porosity decreased slightly for the sample containing 10%wt limestone and increased at a replacement level of 20%wt of limestone.

Generally, the MIP results for the samples containing dolomite and limestone correlate well with the compressive strength results (Figure 2). Samples in which a compressive strength increase was observed for either dolomite or limestone addition compared to the 100CM samples also showed a reduction in the porosity.

AFm AND AFt

XRD

Figure 4 shows the XRD patterns for the various samples cured at 20 °C after 1, 28 and 90 days.

After 28 and 90 days, the ettringite stabilization effect could be observed in all samples containing carbonates when compared with the 100CM sample regardless of the curing temperature, though

95CM5D did show a minor ettringite peak at 38 °C. The addition of a carbonate source to the system increased the CO_2/SO_3 ratio and this meant the carbonate AFm phases, either monocarbonate (11.7 °2θ) or hemicarbonate (10.8 °2θ), were the stable AFm phases instead of monosulphate (9.9 °2θ). Consequently, ettringite (9.1 °2θ) did not transform to monosulphate after the sulphate depletion.

After 1 day, this effect was less obvious because the ettringite peak in the 100CM sample was still present. However, samples containing carbonates, especially limestone, showed higher and sharper ettringite peaks than samples without. In addition to the sulphate-containing phases, after 1 day, the limestone samples showed small traces of monocarbonate peaks and samples containing dolomite showed humps of hemicarbonate.

The trends observed for samples cured at 20 °C after 28 and 90 days were similar to each other, and are therefore described together here. The type of carbonate AFm phase changed with the various replacement levels and the different carbonates used. All samples containing limestone showed clear monocarbonate peaks. At replacement levels of 5%wt, broad peaks of hemicarbonate were also detected, but these disappeared at higher replacement levels. The amount of carbonate AFm phases formed at lower replacement levels seemed to be smaller in samples containing dolomite than in samples containing limestone. In the samples containing dolomite, the types of carbonate AFm and their amount changed more gradually with the level of replacement. In samples containing 5%wt of dolomite, broad humps of both hemi- and monocarbonate were detectable. The monocarbonate peak increased in height and became sharper with higher dolomite additions, while the hemicarbonate peak decreased until it disappeared at 20%wt dolomite addition.

The ettringite peak developed in a similar way to the monocarbonate peak in the samples cured at 20 °C. Samples containing limestone generally showed slightly higher and sharper peaks of

ettringite than samples containing dolomite. However, the ettringite peaks increased in samples containing dolomite with increasing replacement levels.

The phase assemblages detected for the various binder compositions also varied with the curing temperatures. Figure 5 shows the XRD plots for the samples cured for 90 days at the various curing temperatures.

At 5 °C the AFm phases detected were the same as at 20 °C, but their peaks seemed slightly higher and sharper at 20 °C than at 5 °C.

At the highest curing temperature (38 °C), the type of carbonate AFm phases detected in samples containing limestone differed from the samples cured at 5 °C and 20 °C. In the 38 °C samples, the monocarbonate peak decreased and hemicarbonate was detected. In the samples containing dolomite, however, hemicarbonate could already be detected at lower curing temperatures, and differences in the phase assemblage are less obvious than in samples containing limestone.

The very sharp and high peak at 9.9 °2θ in the 90CM10D sample cured at 20 °C for 28 days could be due to monosulphate-12H in the light of the peak position. However, in view of the peak shape and the appearance of carbonate AFm phases in the same sample, it seems more likely to be an artefact of the measurement device. This was confirmed by a second measurement of the sample, which did not show this peak. The origin of this artefact is unknown.

TGA

Figure 6 and Figure 7 show the derivate curves of the TG signal (DTG curves) for the 100CM reference and samples where 5%wt or 20%wt of the CM are replaced by a carbonate source at the various curing temperatures.

The DTG graphs can be divided into several sections, in which the decomposition of specific phases can be detected as weight loss. The first peak at around 100 °C is related to the ettringite decomposition and the beginning of C-H-S dehydroxylation. The C-S-H phase decomposes gradually between 40 °C and 600 °C [39] and appears as a polynomial baseline under other peaks in the same temperature range. The region between approx. 150 °C and 400 °C represents the stepwise dehydroxylation of the AFm phases and other lamellar phases, such as hydrotalcite (Ht) [39]. The subsequent sharp peak between approx. 400 °C and 550 °C is related to the decomposition of portlandite (CH). Above 550 °C, carbonates decompose by emitting CO_2[39].

Monosulphate is distinguishable from carbonate AFm peaks by its slightly higher decomposition temperature [39]. The trends observed in the XRD results are generally confirmed by TGA. The samples containing limestone show significantly higher carbonate AFm peaks than samples containing dolomite, especially at lower replacement levels. The TGA signal does not enable differentiation between hemicarbonate and monocarbonate. All samples show a weight loss in the temperature region of hydrotalcite (Ht). This weight loss does not increase in samples containing dolomite compared to the equivalent limestone-containing samples or the 100CM reference. It can potentially be caused by magnesium-containing hydrates formed due to the high magnesium content of the clinker (Table 1). However, no hydrotalcite could be observed with XRD (Figure 4 and Figure 5), probably due to its poor crystallinity and the small amounts present. A weight loss in this temperature region could also be caused by hydrogarnet or brucite. However, we did not observe any peaks of hydrogarnet nor brucite in our samples with XRD, which are normally quite crystalline and should therefore be visible.

At a replacement level of 5%wt (Figure 6), the samples containing dolomite and limestone show noticeable differences in the relative quantities of AFm and Aft phases. The samples containing 5%wt of limestone show a higher decomposition peak for the ettringite and carbonate AFm

phases than samples containing 5%wt of dolomite. Although this difference is observable at all curing temperatures, its magnitude decreases with increasing curing temperatures.

When 20%wt of the composite cement was replaced with either dolomite or limestone, the DTG curves observed are more alike (Figure 7) than at the replacement level of 5%wt. The samples containing 20%wt of limestone show only slightly higher decomposition peaks for the carbonate AFm phases and AFt than the samples containing 20%wt of dolomite when cured at 5 °C (Figure 7a). At the curing temperature of 38 °C, there are no differences between the samples containing 20%wt of dolomite or limestone (Figure 7c).

BOUND WATER AND PORTLANDITE CONTENT

The amount of bound water and portlandite content for samples with various replacement levels of either dolomite or limestone and the various curing temperatures are plotted in Figure 8a) and Figure 9a) relative to the dry binder weight. In Figure 8b) and Figure 9b) these results are plotted relative to the clinker content.

First, we describe and discuss the results for the samples cured at 20 °C. Any differences in the results for the other curing temperatures are discussed afterwards.

In the case of limestone at 5%wt replacement level, the amount of bound water per dry binder weight was higher than the 100CM sample. At higher replacement levels, the amount of bound water decreased again. This is in line with findings reported for the addition of limestone to Portland cement containing fly ash [24,25]. At a replacement level of 5%wt, the amount of bound water increased compared to samples without limestone addition due to the formation of carbonate AFm phases and the stabilization of ettringite, as explained in the introduction. At

higher replacement levels, the *dilution effect* of replacing the most reactive part with a less-reactive material resulted in a decrease in the amount of bound water.

In the case of dolomite addition, the increase in bound water normalized to the dry binder weight shifted to higher replacement levels (10%wt) and was less pronounced than with limestone addition.

When the bound water is normalized to the clinker content, dilution effects are erased. The amount of bound water normalized to the clinker content increases for all replacement levels of either dolomite or limestone. This way of plotting depicts the enhancement of the clinker reaction due to the *filler effect* when carbonates are added, as described in the introduction.

The portlandite content normalized to the dry binder weight decreased for all replacement levels of either dolomite or limestone. This can be explained by the *dilution effect* of adding a less-reactive material to the system as explained in the introduction.

When the portlandite content is normalized to the clinker content at 5%wt replacement with either dolomite or limestone, a drop in the values is observed. This drop can probably be explained by the formation of hemicarbonate which consumes portlandite [7,8,13,24,40] and an increased reaction of metakaolin when dolomite or limestone is added [41]. At higher replacement levels than 5%wt, the values slightly increase again in the case of limestone, and again this can be explained by the *filler effect* of adding carbonates to cementitious materials. The enhancement of the clinker reaction produces more portlandite, whereas the enhancement of the metakaolin reaction reduces the portlandite content. Therefore, the observed increase in the portlandite content is only minor, while the increase in bound water is significantly higher.

In the case of dolomite addition, however, the portlandite content normalized to the clinker content continues to decrease even at higher replacement levels. Samples containing dolomite also show an increase in the bound water normalized to the clinker content, so this drop cannot be explained by the dolomite failing to promote the clinker reaction. Moreover, the replacement levels are the same for samples containing dolomite as for samples containing limestone, where a slight increase in the portlandite content is observed. Therefore, the decrease in portlandite content normalized to the clinker content observed in samples containing dolomite should be due to the reaction of dolomite itself, which is reported to consume portlandite in model systems [17,23]. However, further research on the reaction of dolomite in cementitious systems, where no brucite but carbonate AFm phases or hydrotalcite are formed, is needed to verify this.

The effect of the various curing temperatures is similar in all plots of either bound water or portlandite content. Samples cured at 5 °C show the highest bound water and portlandite content and with increasing curing temperatures, the values decrease. For the portlandite content, this trend can be explained by the enhanced pozzolanic reaction of the metakaolin, which consumes portlandite. This is why the samples cured at the highest temperatures (38 °C) show the lowest portlandite content. The effect on decreasing bound water with increasing curing temperatures has been ascribed to the densification of the C-S-H phase at higher temperatures, which is connected with a decrease in its structural water [42,43]. This decrease in the water content of the C-S-H phase in the samples cured at elevated temperatures affects the bound water content more than a possible enhancement of the clinker hydration.

For the samples containing dolomite or limestone, the results for bound water content and portlandite content were generally quite similar for replacement levels >10%wt. However, when only 5%wt of the Portland metakaolin cement is replaced by dolomite, the bound water content is significantly reduced. This is visible both at the various curing temperatures shown in Figure 8 and for the various curing times shown in Figure 10 for 20 °C. Moreover, this difference in bound

449 water content is most obvious in samples cured at low temperatures (5 °C) and decreases with
450 increasing curing temperatures. This correlates with the compressive strength results and the
451 observed phase assemblages, indicating that dolomite has a lower reactivity than limestone.
452
453 **THERMODYNAMIC MODELLING**
454
455 Thermodynamic modelling was used to confirm the hydrate phase assemblages observed by XRD
456 and TGA and to relate them to the degree of reaction of dolomite or limestone. The effect of the
457 addition of 5%wt of dolomite or limestone was therefore modelled to find the degree of reaction
458 of the two carbonate sources at complete hydration of the clinker and metakaolin.
459
460 Figure 11 shows the modelled phase assemblage for 5%wt of dolomite and limestone addition
461 depending on the degree of reaction of the carbonate source. The figure shows that the addition
462 of 5%wt of either carbonate source results in a similar phase assemblage.
463
464 When the carbonate source has not dissolved at all, hydrogarnet, C-S-(A)-H phase, monosulphate,
465 portlandite and hydrotalcite are the stable hydration products. As soon as the carbonate source
466 reacts, hemicarbonate becomes stable and increases in volume as the degree of reaction increases
467 in both cases. Simultaneously with the increase in hemicarbonate, monosulphate decreases and,
468 after approx. 7% of reaction, ettringite becomes stable. At a certain degree of reaction,
469 monocarbonate becomes the stable carbonate AFm phase. Its volume increases simultaneously
470 with the decrease in the volume of hemicarbonate that started the moment monocarbonate
471 became stable.
472
473 Differences between dolomite and limestone are only visible in the volume of specific hydrates. In
474 the simulation with dolomite more hydrotalcite is predicted, whereas in the limestone simulation
475 more monocarbonate is predicted. The higher volume for the secondary calcite in the sample

containing dolomite than in the sample containing limestone is expected because calcite is a product of the dedolomitization reaction.

DISCUSSION OF THE EFFECT OF DOLOMITE ADDITION

The effect of dolomite addition at 20 °C

The addition of limestone leads to the stabilization of ettringite and the formation of additional carbonate AFm phases [6,7]. The effects on the phase assemblage reported for limestone addition to aluminium-rich cements [24–28] can also be shown for dolomite addition to Portland metakaolin cement. This suggests that the two carbonate sources affect the system in a similar way.

However, the phase assemblage in the samples containing dolomite differed over the various replacement levels from those containing limestone. At a low replacement level (5%wt), there was a difference in the type of carbonate-AFm phases formed. In samples containing dolomite, both hemi- and monocarbonate were formed, while the carbonate-AFm phase formed in samples containing limestone was almost entirely monocarbonate. However, at higher replacement levels, this difference disappeared. In all samples containing 20%wt of either carbonate source, monocarbonate was the main carbonate AFm phase formed.

This could be due to the different rates of reaction of dolomite and limestone. Since limestone is more reactive than dolomite [21], it provides CO_2 to the system faster. After 28 days, sufficient limestone was able to react with the aluminium and form monocarbonate. The lower reactivity of dolomite reduces the CO_2/Al_2O_3 ratio present in the system, which promotes the formation of hemicarbonate over monocarbonate [13]. It should be noted, that the differences in the type of the AFm phase formed are amplified due to the metakaolin content in the composite cement,

503 which is decreasing the CO_2/Al_2O_3 ratio in the system. Moreover, dolomite contains more CO_2 than
504 limestone on a weight basis (Table 1), a slightly smaller amount of dolomite has to react to deliver
505 the same amount of CO_2 to the system and consequently form similar carbonate AFm phases.
506
507 The difference in reactivity is indicated by comparing results from the thermodynamic modelling
508 and experimental results for the 95CM5D and 95CM5L samples at 20 °C. Both dolomite and
509 limestone result in the same hydrate phase assemblage at high degrees of reaction with only
510 minor differences in their relative quantity. Consequently, the differences in the phase assemblage
511 observed at low replacement levels must be due to the difference in the degree of reaction present
512 in dolomite and limestone at 28 and 90 days. The areas highlighted in both plots (dotted
513 rectangles) represent the experimentally observed phase assemblage, i.e. the area of
514 hemicarbonate transformation to monocarbonate in these samples. They show that for limestone
515 there is a larger area of influence compared to dolomite, probably indicating a higher degree of
516 reaction. A direct comparison is, however, not possible, due to the similar solubilities of hemi- and
517 monocarbonate [7].
518
519 It should be noted that the modelling assumed complete reaction of the clinker and the
520 metakaolin. This is unlikely after 90 days in the experimentally investigated samples, especially
521 in case of the clinker. The impact of this assumption on the results is probably an overestimation
522 of the amount of hydrates formed, this is visible in the high amounts of hydrogarnet predicted by
523 the thermodynamic model, which could not be observed experimentally. The relative stabilities
524 between hemi- and monocarbonate should not be affected because they depend on the degree of
525 reaction of the carbonate source. Moreover, the purpose of these simulations is to compare
526 samples containing dolomite and limestone, and the same assumptions were made in both
527 samples.
528

529 Furthermore, it should be noted that the differences in the reactivity of these two materials would
530 probably have been enhanced if dolomite and limestone of the same fineness had been used.
531
532 At higher replacement levels of dolomite, more carbonate is available in the system, which
533 increases the CO_2/Al_2O_3 ratio. The higher CO_2/Al_2O_3 ratio led to the formation of monocarbonate
534 in samples containing dolomite at high replacement levels [13]. Consequently, at replacement
535 levels of 20%wt, the carbonate AFm phase assemblages were generally quite similar for samples
536 containing dolomite and limestone, as previously reported by Zajac et al. [19].
537
538 At low replacement levels of limestone, only monocarbonate formed despite the considerable
539 metakaolin content of the samples. This suggests fast kinetics of the limestone reaction. We do not
540 think that carbonation due to sample preparation could explain the monocarbonate stabilization
541 because hemicarbonate peaks were observed in the samples containing dolomite.
542
543 The addition of dolomite and limestone to calcined-clay containing Portland composite cement
544 affects not only the phase assemblages in a similar way but also the compressive strength
545 development. The addition of dolomite increased the compressive strength up to a replacement
546 level of 10%wt. This effect can be attributed to the above-mentioned effect of ettringite
547 stabilization and the formation of carbonate AFm phases. Ettringite requires more space than
548 monosulphate, so it reduces the porosity of the resulting hydrated cement and increases its
549 compressive strength [6,7]. Because these effects are amplified when sufficient amounts of
550 aluminium are provided to the system [24–28], we used a Portland metakaolin cement instead of
551 a plain Portland cement.
552
553 However, there are differences between samples containing dolomite and those containing
554 limestone.
555

556 The strength increase due to the carbonate addition was less pronounced for samples containing
557 dolomite than for samples containing limestone. The optimum replacement level with the highest
558 compressive strength was also different for samples containing dolomite and limestone.
559 According to the results reported by De Weerdt et al. [24,25], the optimum addition of limestone
560 to the composite cement is around 5%wt. For the samples containing dolomite, the maximum
561 compressive strength was achieved by 5%wt addition after 28 days and for 10%wt addition after
562 90 days of hydration.
563
564 Moreover, at lower replacement levels, samples containing dolomite showed a lower compressive
565 strength than samples containing limestone. This effect might also be explained by the slower rate
566 of reaction of dolomite. It delivers fewer carbonate ions to the system, so the total amount of
567 carbonate AFm phases and ettringite that can be formed at early ages is smaller. This was
568 confirmed by TGA, which showed that the amount of ettringite and carbonate AFm phases formed
569 at a replacement level of 5%wt was significantly lower in samples containing dolomite than in
570 samples containing limestone. Moreover, the bound water content of samples containing 5%wt of
571 dolomite was lower than in samples containing 5%wt of limestone.
572
573 However, these differences were levelled out at higher replacement levels (10%wt). For the
574 highest addition levels tested, dolomite samples showed similar or slightly higher compressive
575 strength values. Such higher compressive strength values for higher replacement levels of
576 dolomite have been reported before [44,45]. The amount of carbonate AFm phases formed and
577 the bound water content were also similar at the high replacement level of 20%wt. It seems,
578 therefore, that adding sufficient amounts of dolomite to the system can overcome the effect of the
579 lower rate of reaction of dolomite and the accompanying dilution effect of replacing cement with
580 a less reactive material.
581

582 The compressive strength results show that relatively high amounts of CM can be replaced by the
583 carbonates without impairing compressive strength. However, in the case of OPC, the addition of
584 >5%wt of carbonates normally results in a drop in compressive strength [24,25]. This can be
585 explained by the fact, that the reaction of metakaolin tends to refine the microstructure of the
586 cement paste [46,47], and therefore might limit itself from further reaction [41]. The addition of
587 either dolomite or limestone provides additional space [16,45] and water, which might allow the
588 metakaolin to react further [41]. This is also visible in our results of the portlandite and bound
589 water content (Figure 8 and Figure 9). Consequently, more pore space will be filled with additional
590 C-S-H. This effect might be counteracting a strength decrease due to dilution partially and allow
591 relatively high replacement levels without impairing the compressive strength.
592
593 It should be noted that the dolomite used was very fine compared to the limestone used. This
594 should be kept in mind when the rate of reaction of the two carbonate sources is discussed on the
595 basis of the present investigation. Differences resulting from the reactivity of dolomite being
596 lower than that of limestone might be greater with natural and coarser dolomite rock [48].
597 Moreover, the smaller particle size distribution of the dolomite used compared to the limestone
598 used might have affected the compressive strength results due to improved particle packing.
599 However, De Weerdt et al. showed that varying the fineness of limestone additions between
600 362 m^2/kg and 812 m^2/kg did not significantly affect the compressive strength of Portland fly-ash
601 cements [30]. So although the dolomite used in this study had a fineness of approx. 1056 m^2/kg,
602 we think this would have no significant effect. Lawrence et al. concluded that a compressive
603 strength increase with the addition of fine limestone was due to the enabling of heterogeneous
604 nucleation (filler effect) rather than any particle packing effect [49]. We think this effect is also
605 likely to apply for both dolomite and for the metakaolin [50,51], which was already present in the
606 CM before any carbonate addition.
607

608 It can be concluded that the reactions that affect the system when dolomite or limestone is added
609 to Portland metakaolin cement are similar. An apparent strength increase due to the addition of
610 carbonates can only be observed when the carbonates have reacted (28 and 90 days). In these
611 samples, the fine dolomite investigated appears to be able to replace approx. 10%wt of calcined
612 clay-containing composite cement without impairing its compressive strength.
613

614 **The effect of dolomite addition at various curing temperatures**

615 The various curing temperatures tested had different effects on the compressive strength
616 development of the composite cement with dolomite addition as opposed to limestone.
617

618 At low curing temperatures (5 °C), the dolomite samples show consistently lower compressive
619 strength values than the samples containing limestone at replacement levels < 20%wt. This can
620 also be explained by the different rates of reaction of dolomite and limestone, and their differing
621 ability to provide CO_2 to the system. The XRD results show a different phase assemblage, and TGA
622 results show the formation of a smaller amount of AFt and carbonate AFm phases, as described
623 for the 20 °C samples at low replacement levels. These observed differences might explain the
624 overall lower compressive strength of samples containing dolomite compared to those containing
625 limestone.
626

627 At each higher level of curing temperature from 5 °C to 38 °C, the differences between samples
628 containing dolomite or limestone decrease. As a result, at 38 °C, and with the exception of the
629 5%wt replacement level, the dolomite and limestone samples ended up showing similar results
630 in compressive strength for all replacement levels. The increase in strength of dolomite samples
631 at elevated temperatures has been reported previously [19,45] and indicates an enhanced rate of
632 reaction of the dolomite at these temperatures [19,23,45]. So, the lower compressive strength of
633 the samples containing dolomite at some replacement levels seems to be counteracted by
634 increasing the curing temperature.

The phase assemblages of samples containing dolomite and limestone also develop differently with increased curing temperatures. XRD analysis showed that more hemicarbonate was formed at higher temperatures in samples containing limestone. Enhanced metakaolin reaction at higher temperatures reduced the CO_2/Al_2O_3, which favours the formation of hemicarbonate [13]. This increased aluminium content in the pore solution at higher curing temperatures was shown by Deschner et al. for cement containing fly ash [52].

However, the samples containing dolomite did not show significant changes in the hemicarbonate-to-monocarbonate ratio at elevated temperatures (38 °C) compared to the samples cured at 20 °C, because hemicarbonate is already detected at low temperatures. The lower reactivity of dolomite compared to limestone provides a low CO_2/Al_2O_3 ratio at all temperatures, and no phase changes occur when the ratio is lowered even further.

As a result, the phase assemblages for samples containing dolomite and limestone are very similar at elevated temperatures. This was confirmed using TGA, where samples containing dolomite and limestone also showed similar weight losses in the AFt and carbonate AFm temperature range for higher curing temperatures (38 °C).

We can summarize that dolomite and limestone additions to Portland metakaolin cement result in similar compressive strength and similar phase assemblages as long as similar degrees of reaction are achieved. The lower reactivity of dolomite can be counteracted by using increased curing temperatures.

Long-term compressive strength development and questions of durability are possible topics for further research on dolomite as a valid SCM. Moreover, the dolomite used in this study is only one

example of a reactive carbonate not covered by EN 197-1 [2]. There are many other carbonate sources which could prove useful as a replacement for pure limestone.

CONCLUSION

Portland metakaolin cement with various replacement levels of up to 20%wt with either dolomite or limestone were investigated with regard to their compressive strength and phase assemblage when cured at 5 °C, 20 °C and 38 °C for up to 90 days.

- Dolomite addition affects Portland metakaolin cement in a similar way to limestone addition. Both result in the formation of additional carbonate AFm phases and ettringite stabilization and either can be used to replace part of the Portland metakaolin cement without impairing its compressive strength at 90 days. At low levels of addition, they can even enhance this strength. In the case of the dolomite, the positive effect was not visible after 90 days of reaction at 5 °C but seemed to be amplified when cured at 38 °C.
- Thermodynamic modelling in combination with experimental determination of phase assemblages indicate a lower degree of reaction for dolomite addition than for limestone when cured at 20 °C for 90 days. This results in a lower ability to deliver CO_2 to the system at 90 days. This was confirmed experimentally by the slight differences in the type and amount of AFm and Aft phases observed at low replacement levels between samples containing dolomite and limestone.
- A similar degree of reaction of dolomite and limestone can be achieved, however, by increasing the curing temperature. At 38 °C the similar phase assemblage and compressive strength indicate a similar degree of reaction.

ACKNOWLEDGEMENTS

The authors would like to acknowledge the industrial PhD programme of the Norwegian Research Council (Project: 241637) and the Heidelberg Technology Center for their financial support. We are also grateful for the help and assistance of the Norcem AS concrete laboratory with the compressive strength tests.

691

692 **References**

693 [1] B. Lothenbach, K.L. Scrivener, R.D. Hooton, Supplementary cementitious materials, Cem
694 Concr Res 41 (12) (2011) 1244–1256.
695 [2] EN 197-1, Cement, Part I: Composition, specifications and conformity criteria for common
696 cements, European Committee for Standardization, Brussels, 2011.
697 [3] J. Péra, S. Husson, B. Guilhot, Influence of finely ground limestone on cement hydration,
698 Cement and Concrete Composites 21 (2) (1999) 99–105.
699 [4] I. Soroka, N. Stern, Calcareous fillers and the compressive strength of Portland cement, Cem
700 Concr Res 6 (3) (1976) 367–376.
701 [5] L. Nicoleau, Accelerated growth of calcium silicate hydrates: Experiments and simulations,
702 Cem Concr Res 41 (12) (2011) 1339–1348.
703 [6] T. Matschei, B. Lothenbach, F.P. Glasser, The role of calcium carbonate in cement hydration,
704 Cem Concr Res 37 (4) (2007) 551–558.
705 [7] B. Lothenbach, G. Le Saout, E. Gallucci, K.L. Scrivener, Influence of limestone on the
706 hydration of Portland cements, Cem Concr Res 38 (6) (2008) 848–860.
707 [8] V.L. Bonavetti, V.F. Rahhal, E.F. Irassar, Studies on the carboaluminate formation in
708 limestone filler-blended cements, Cem Concr Res 31 (6) (2001) 853–859.
709 [9] R.F. Feldmann, V.S. Ramachandran, P.J. Sereda, Influence of $CaCO_3$ on the Hydration of
710 $3CaO{\cdot}Al_2O_3$, J Am Ceram Soc 48 (1) (1965) 25–30.
711 [10] J. Bensted, Some hydration investigations involving Portland cement - effect of calcium
712 carbonate substitution of gypsum, World Cement Technology 11 (8) (1980) 395–406.
713 [11] A.P. Barker, H.P. Cory, The early hydration of limestone-filled cements, in: R.N. Swamy (Ed.),
714 Blended Cements in Construction, Taylor & Francis, Sheffield, UK, 1991, pp. 107–124.
715 [12] K. Ingram, M. Polusny, K. Daugherty, W. Rowe, Carboaluminate reactions as influenced by
716 limestone additions, in: P. Klieger, R.D. Hooton (Eds.), Carbonate Additions to Cement:
717 ASTM STP 1064, American Society for Testing and Materials, Philadelphia, PA, 1990,
718 pp. 14–23.
719 [13] T. Matschei, B. Lothenbach, F.P. Glasser, The AFm phase in Portland cement, Cem Concr Res
720 37 (2) (2007) 118–130.
721 [14] P. Hawkins, P.D. Tennis, R.J. Detwiler, The Use of Limestone in Portland Cement: A State-of-
722 the-Art Review., Portland Cement Association (2003).
723 [15] S. Schöne, W. Dienemann, E. Wagner, Portland Dolomite Cements as Alternative to Portland
724 Limestone Cements, in: Proceedings of the 13th International Congress on the Chemistry of
725 Cement, Madrid, Madrid, 2011.

[16] M. Zajac, W. Dienemann, G. Bolte, Comparative experimental and virtual investigations of the influence of calcium and magnesium carbonates on reacting cement, in: Proceedings of the 13th International Congress on the Chemistry of Cement, Madrid, Madrid, 2011.
[17] S. Galí, C. Ayora, P. Alfonso, E. Tauler, M. Labrador, Kinetics of dolomite-portlandite reaction: Application to Portland cement concrete, Cem Concr Res 31 (6) (2001) 933–939.
[18] E. Garcia, P. Alfonso, M. Labrador, S. Galí, Dedolomitization in different alkaline media: Application to Portland cement paste., Cem Concr Res 33 (9) (2003) 1443–1448.
[19] M. Zajac, S.K. Bremseth, M. Whitehead, M. Ben Haha, Effect of $CaMg(CO_3)_2$ on hydrate assemblages and mechanical properties of hydrated cement pastes at 40 °C and 60 °C, Cem Concr Res 65 (2014) 21–29.
[20] J.W. Morse, R.S. Arvidson, The dissolution kinetics of major sedimentary carbonate minerals, Earth-Science Reviews 58 (1–2) (2002) 51–84.
[21] O.S. Pokrovsky, S.V. Golubev, J. Schott, A. Castillo, Calcite, dolomite and magnesite dissolution kinetics in aqueous solutions at acid to circumneutral pH, 25 to 150 °C and 1 to 55 atm pCO_2: New constraints on CO_2 sequestration in sedimentary basins, Chemical Geology 265 (1–2) (2009) 20–32.
[22] L. Chou, R.M. Garrels, R. Wollast, Comparative study of the kinetics and mechanisms of dissolution of carbonate minerals, Chemical Geology 78 (3-4) (1989) 269–282.
[23] X. Zhang, F.P. Glasser, K.L. Scrivener, Reaction kinetics of dolomite and portlandite, Cem Concr Res 66 (2014) 11–18.
[24] K. De Weerdt, H. Justnes, K.O. Kjellsen, E. Sellevold, Fly ash-limestone ternary composite cements: synergetic effect at 28 days, Nordic Concrete Research 42 (2) (2010) 51–70.
[25] K. De Weerdt, K.O. Kjellsen, E. Sellevold, H. Justnes, Synergy between fly ash and limestone powder in ternary cements, Cement and Concrete Composites 33 (1) (2011) 30–38.
[26] M. Antoni, J. Rossen, F. Martirena, K.L. Scrivener, Cement substitution by a combination of metakaolin and limestone, Cem Concr Res 42 (12) (2012) 1579–1589.
[27] G. Puerta-Falla, M. Balonis, G. Le Saout, N. Neithalath, G. Sant, The Influence of Metakaolin on Limestone Reactivity in Cementitious Materials, in: Calcined Clays for Sustainable Concrete: Proceedings of the 1st International Conference on Calcined Clays for Sustainable Concrete, Lausanne, Switzerland, 2015, pp. 11–19.
[28] D. Nied, C. Stabler, M. Zajac, Assessing the synergistic effect of limestone and metakaolin, in: Calcined Clays for Sustainable Concrete: Proceedings of the 1st International Conference on Calcined Clays for Sustainable Concrete, Lausanne, Switzerland, 2015, pp. 245–251.
[29] EN 196-1, Methods of testing cement, PartI: Determination of strength, European Committee for Standardization, Brussels, 2005.

[30] K. De Weerdt, E. Sellevold, K.O. Kjellsen, H. Justnes, Fly ash–limestone ternary cements: effect of component fineness, Advances in Cement Research 23 (4) (2011) 203–214.
[31] B. Lothenbach, F. Winnefeld, Thermodynamic modelling of the hydration of Portland cement, Cem Concr Res 36 (2) (2006) 209–226.
[32] D. Kulik, GEM-Selektor v.3.3, available at available at: http://gems.web.psi.ch/.
[33] D.A. Kulik, T. Wagner, S.V. Dmytrieva, G. Kosakowski, F.F. Hingerl, K.V. Chudnenko, U.R. Berner, GEM-Selektor geochemical modeling package: Revised algorithm and GEMS3K numerical kernel for coupled simulation codes, Comput Geosci 17 (1) (2013) 1–24.
[34] T. Wagner, D.A. Kulik, F.F. Hingerl, S.V. Dmytrieva, GEM-Selektor geochemical modeling package: TSolMod library and data interface for multicomponent phase models, The Canadian Mineralogist 50 (5) (2012) 1173–1195.
[35] Thermodynamic database, provided by EMPA, available at: https://www.empa.ch/web/s308/thermodynamic-data.
[36] D.A. Kulik, Improving the structural consistency of C-S-H solid solution thermodynamic models, Cem Concr Res 41 (5) (2011) 477–495.
[37] B.Z. Dilnesa, B. Lothenbach, G. Renaudin, A. Wichser, D. Kulik, Synthesis and characterization of hydrogarnet $Ca_3(Al_xFe_{1-x})_2(SiO_4)_y(OH)_{4(3-y)}$, Cem Concr Res 59 (2014) 96–111.
[38] B. Lothenbach, T. Matschei, G. Möschner, F.P. Glasser, Thermodynamic modelling of the effect of temperature on the hydration and porosity of Portland cement, Cem Concr Res 38 (1) (2008) 1–18.
[39] B. Lothenbach, P. Durdzinski, K. De Weerdt, Thermogravimetric Analysis, in: K.L. Scrivener, R. Snellings, B. Lothenbach (Eds.), A Practical Guide to Microstructural Analysis of Cementitious Materials, CRC Press Taylor & Francis Group, Boca Raton, 2015, pp. 177–211.
[40] H. Hirao, K. Yamada, S. Hoshino, H. Yamashita, The Effect of Limestone Powder Addition on the Optimum Sulfate Levels of Cement Having Various Al_2O_3 Contents, in: Proceedings of the 12th International Congress on the Chemistry of Cement, Montreal, Montreal, 2007.
[41] W. Kunther, Z. Dai, J. Skibsted, Thermodynamic modeling of hydrated white Portland cement–metakaolin–limestone blends utilizing hydration kinetics from ^{29}Si MAS NMR spectroscopy, Cem Concr Res 86 (2016) 29–41.
[42] E. Gallucci, X. Zhang, K.L. Scrivener, Effect of temperature on the microstructure of calcium silicate hydrate (C-S-H), Cem Concr Res 53 (2013) 185–195.
[43] B. Lothenbach, F. Winnefeld, C. Alder, E. Wieland, P. Lunk, Effect of temperature on the pore solution, microstructure and hydration products of Portland cement pastes, Cem Concr Res 37 (4) (2007) 483–491.

[44] O. Mikhailova, G. Yakovlev, I. Maeva, S. Senkov, Effect of Dolomite Limestone Powder on the Compressive Strength of Concrete, Procedia Engineering 57 (2013) 775–780.
[45] J. Xu, D. Lu, Zhang S., K. Ling, Z. Xu, Pore Structures of Mortars with Dolomite and Limestone Powders Cured at Various Temperatures, Journal of the Chinese Ceramic Society 45 (2) (2017) 268–273.
[46] B. Akcay, M.A. Tasdemir, Investigation of Microstructure Properties and Early Age Behavior of Cementitious Materials Containing Metakaolin, in: CONCREEP 10: Mechanics and Physics of Creep, Shrinkage, and Durability of Concrete and Concrete Structures, Vienna, Austria, American Society of Civil Engineers, Reston, VA, 2015, pp. 1468–1475.
[47] M. Frías, J. Cabrera, Pore size distribution and degree of hydration of metakaolin–cement pastes, Cem Concr Res 30 (4) (2000) 561–569.
[48] T. Knudsen, The dispersion model for hydration of Portland cement - I. General concepts., Cem Concr Res 14 (5) (1984) 622–630.
[49] P. Lawrence, M. Cyr, E. Ringot, Mineral admixtures in mortars effect of type, amount and fineness of fine constituents on compressive strength, Cem Concr Res 35 (6) (2005) 1092–1105.
[50] G. Marchetti, V.F. Rahhal, E.F. Irassar, Influence of packing density and water film thickness on early-age properties of cement pastes with limestone filler and metakaolin, Mater Struct 50 (2) (2017) Article: 111.
[51] B. Ilić, V. Radonjanin, M. Malešev, M. Zdujić, A. Mitrović, Study on the addition effect of metakaolin and mechanically activated kaolin on cement strength and microstructure under different curing conditions, Constr Build Mater 133 (2017) 243–252.
[52] F. Deschner, B. Lothenbach, F. Winnefeld, J. Neubauer, Effect of temperature on the hydration of Portland cement blended with siliceous fly ash., Cem Concr Res 52 (2013) 169–181.

OVERVIEW OF TABLES

TABLES

Table 1: XRF results [%wt] and Blaine specific surface area of the clinker, dolomite, limestone, metakaolin and gypsum used.

Oxide	Clinker	Dolomite	Limestone	Metakaolin	Gypsum
SiO_2	20.6	0.01	0.00	52.18	0.02
Al_2O_3	5.6	0.02	0.00	44.92	0.09
TiO_2	0.29	0.00	0.00	1.14	0.00
MnO	0.05	0.00	0.00	0.00	0.00
Fe_2O_3	3.12	0.00	0.00	0.62	0.00
CaO	63.26	30.32	55.87	0.12	32.66
MgO	2.66	21.59	0.21	0.04	0.06
K_2O	1.23	0.00	0.00	0.18	0.01
Na_2O	0.51	0.00	0.00	0.17	0.02
SO_3	1.37	0.00	0.00	0.14	46.47
P_2O_5	0.09	0.00	0.01	0.07	0.00
LOI	-	47.53	43.73	0.29	20.39
Blaine surface area [m^2/kg]	404	1056	482	897	214
Sum (1050 °C)	**98.78**	**99.52**	**99.82**	**99.87**	**99.72**

Table 2: Mineral composition of the dolomite, limestone, metakaolin and gypsum, determined by Rietveld analysis [%wt]. Amounts given in italics are below the limits of quantification (1%wt). The quantification of mullite is questionable due to its low crystallinity.

Mineral name	Mineral formula	Dolomite	Limestone	Metakaolin	Gypsum
Hydromagnesite	$Mg_3(CO_3)_4(OH)_2{\cdot}4H_2O$	-	-	-	-
Calcite	$CaCO_3$	-	100	-	-
Dolomite	$CaMg(CO3)_2$	100	-	-	-
Gypsum	$CaSO_4{\cdot}2H_2O$	-	-	-	93.7
Bassanite	$CaSO_4{\cdot}0.5H_2O$	-	-	-	6.3
Anatase	TiO_2	-	-	*1.2*	-
Mullite	$Al_6Si_2O_{13}$	-	-	*6.1*	-
Muscovite	$KAl_2Si_3AlO_{10}(OH)_2$	-	-	*0.4*	-
Quartz	SiO_2	-	-	*0.7*	-
Amorphous content	-	-	-	91.6	-

Table 3: Mineralogical composition of the clinker used determined by Rietveld analysis [%wt].

Mineral	**%wt**
Alite	59.5
α-Belite	1.4
β-Belite	13.9
Σ Belite	15.3
Aluminate (cub.)	5.3
Aluminate (or.)	3.5
Σ Aluminate	8.8
Ferrite	10.0
Periclase	1.5
Free Lime	0.9
Portlandite	1.2
Aphthitalite	2.4
Arcanite	0.5

Table 4: Overview of the experimental matrix. To all mixes, 2.85%wt of laboratory-grade gypsum was added.

No.	**Name of the mix**	**CM (OPC:MK = 6:1)**	**L**	**D**
1	100CM	100		
2	95CM5L	95	5	
3	90CM10L	90	10	
4	80CM20L	80	20	
5	95CM5D	95		5
6	90CM10D	90		10
7	80CM20D	80		20

OVERVIEW OF FIGURES

884 **FIGURES**

885

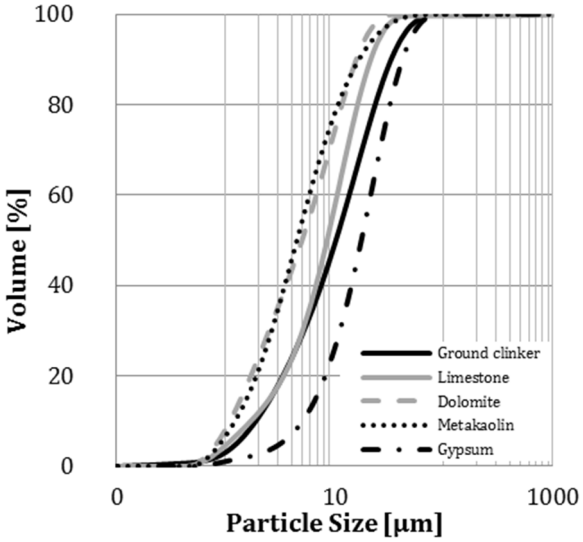

886

887 Figure 1: Particle size distributions of the materials used, determined by laser diffraction.

888

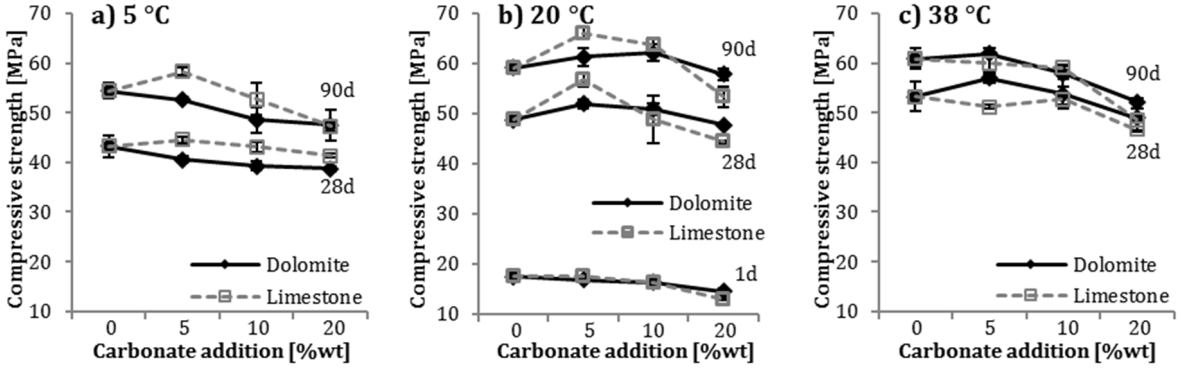

Figure 2: Development of compressive strength for the different carbonate additions and the reference, for samples cured for up to 90 days at a) 5 °C, b) 20 °C, c) 38 °C.

889

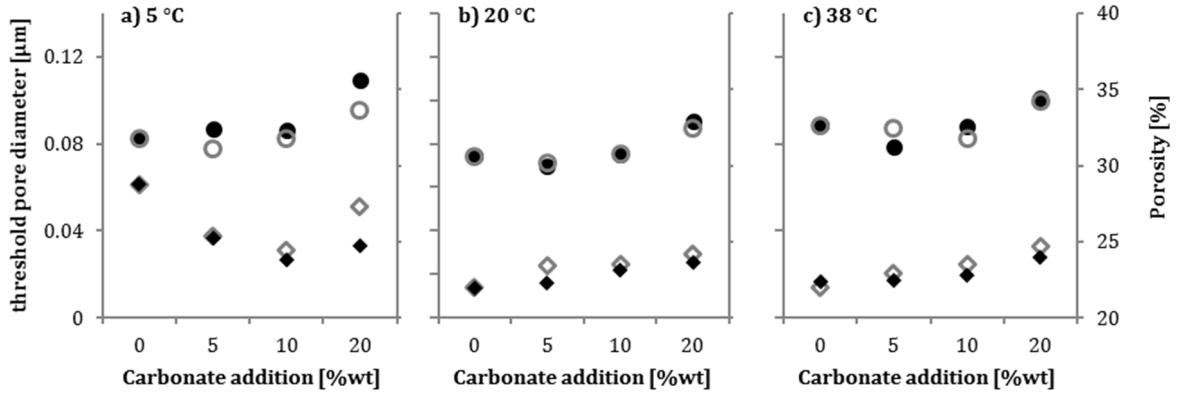

Figure 3: Development of the threshold pore diameter (*diamonds*) and the total intruded volume (*dots*) for samples containing dolomite (*black filled*) or limestone (*grey hollow*) stored at a) 5 °C, b) 20 °C and c) 38 °C at 90 days.

890

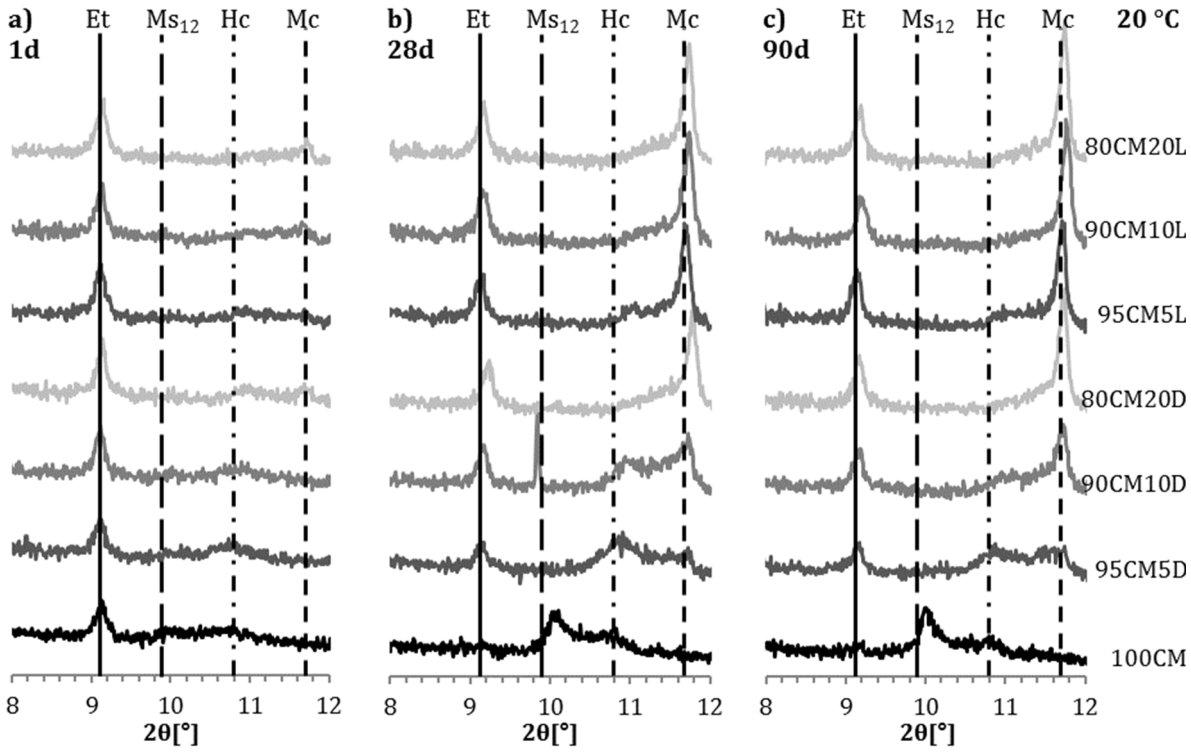

Figure 4: XRD patterns between 8 °2θ and 12 °2θ for the samples investigated after 1 day, 28 days and 90 days of hydration at 20 °C.

891

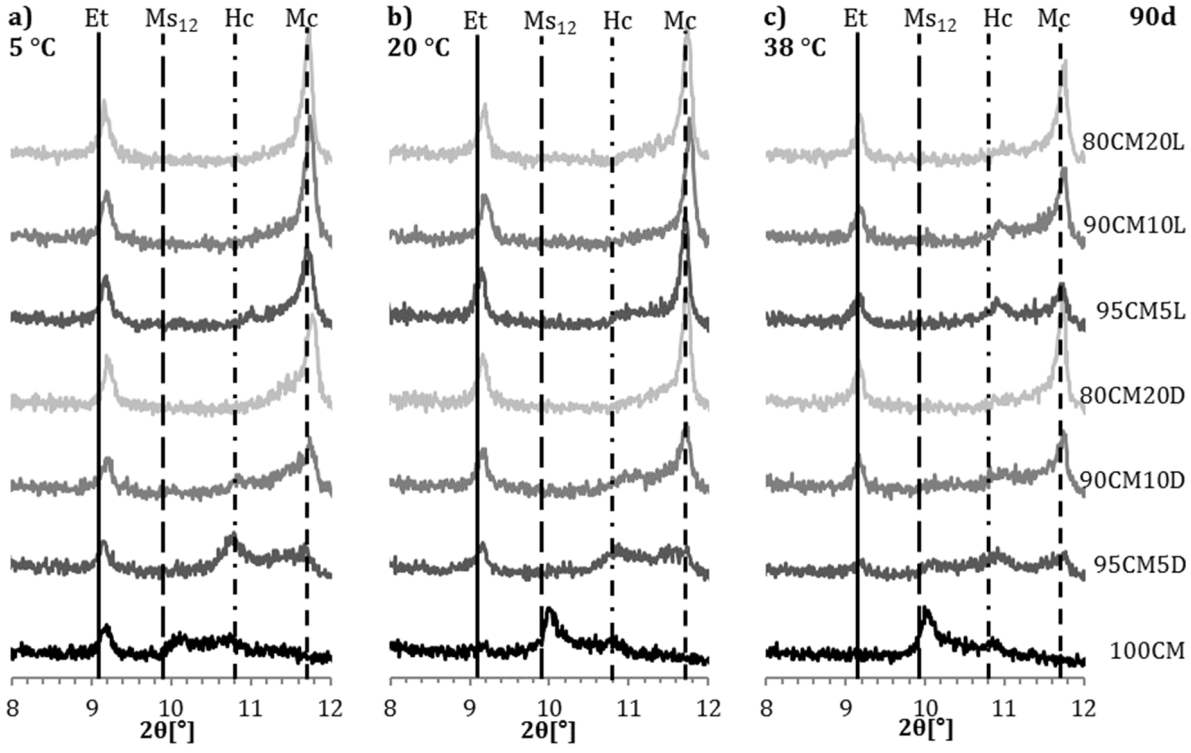

Figure 5: XRD patterns between 8 °2θ and 12 °2θ for the samples investigated after 90 days of hydration, cured at a) 5 °C, b) 20 °C, c) 38 °C.

892

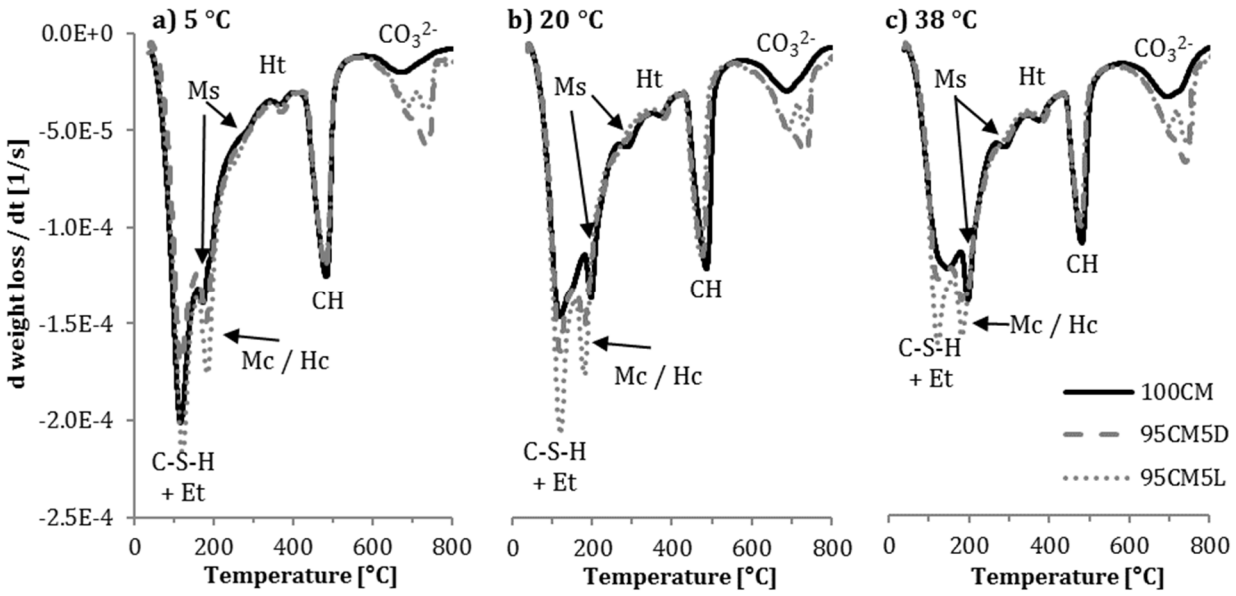

Figure 6: Differential thermogravimetric (DTG) curves for samples cured for 90d with a replacement level of 5%wt cured at a) 5 °C, b) 20 °C and c) 38 °C.

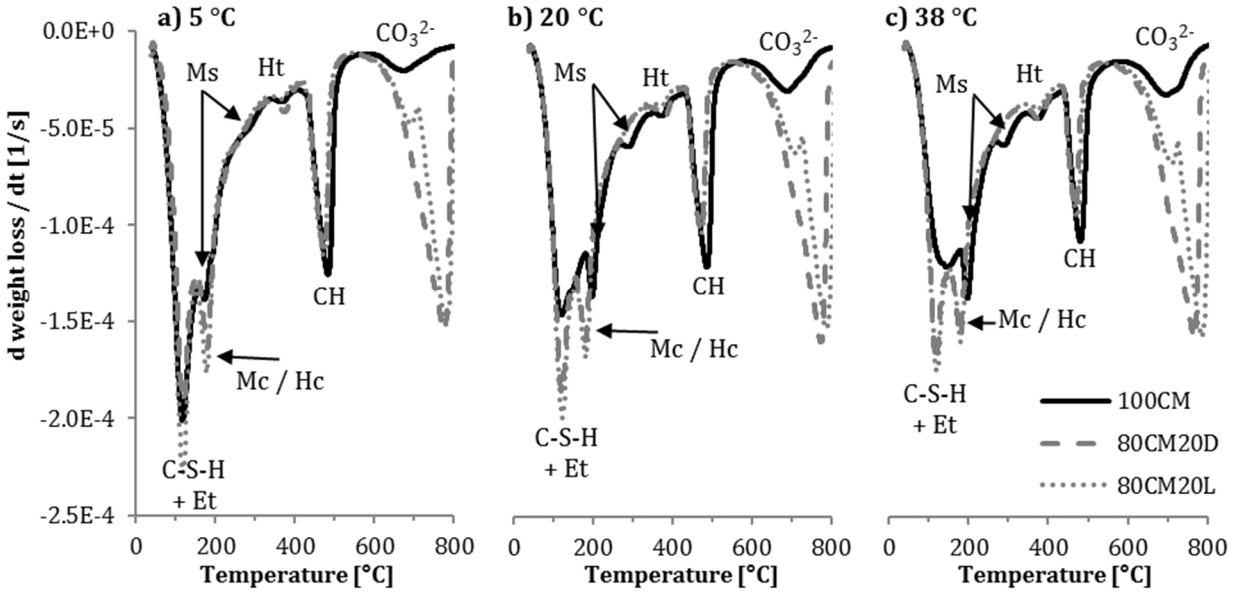

Figure 7: Differential thermogravimetric (DTG) curves for samples cured for 90d with a replacement level of 20%wt cured at a) 5 °C, b) 20 °C and c) 38 °C.

893

894

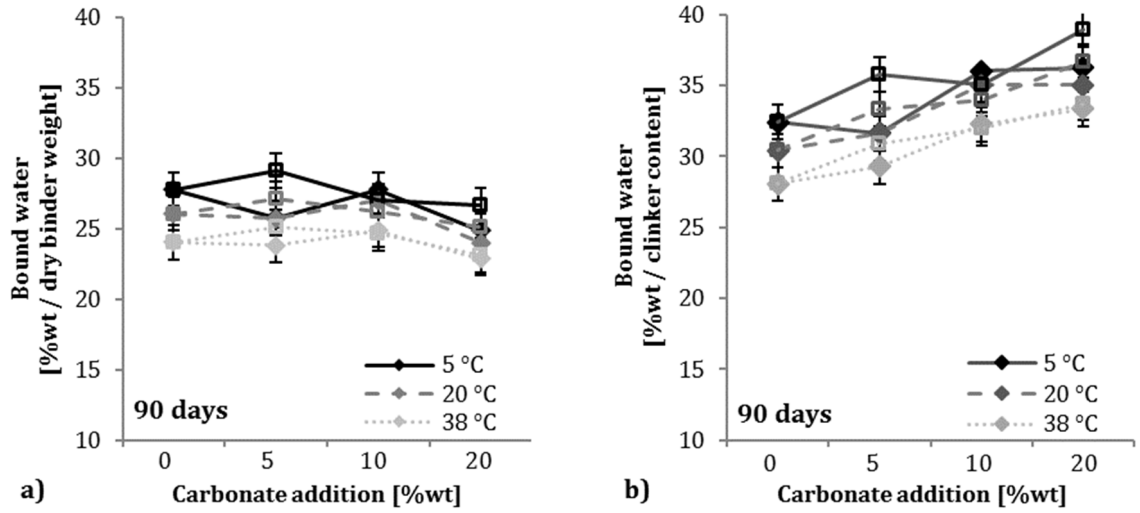

Figure 8: Amount of the bound water for samples containing dolomite (*filled diamonds*) or limestone (*hollow squares*) and the reference (0%wt carbonate addition) cured for 90 days at 5 °C, 20 °C and 38 °C. The results are normalized to the dry binder weight (a) and the clinker content (b).

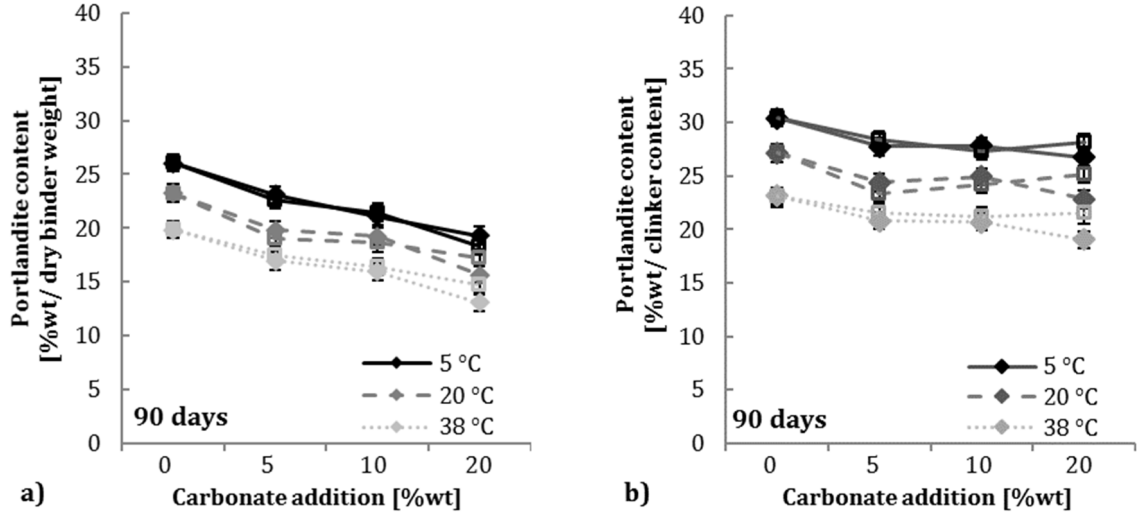

Figure 9: Amount of portlandite for samples containing dolomite (*filled diamonds*) or limestone (*hollow squares*) and the reference (0%wt carbonate addition) cured for 90 days at 5 °C, 20 °C and 38 °C. The results are normalized to the dry binder weight (a) and the clinker content (b).

895

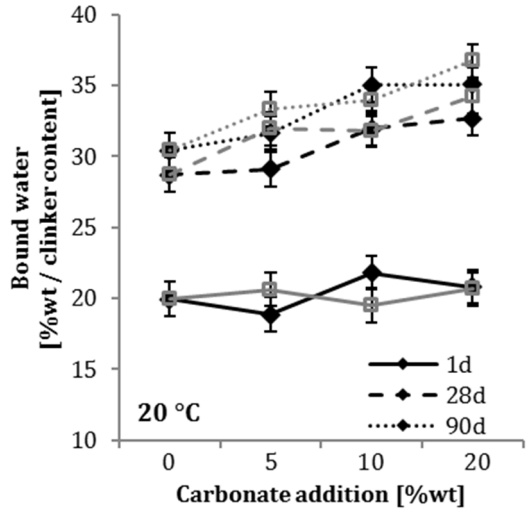

Figure 10: Amount of bound water for samples with various additions of dolomite *(black diamonds)* or limestone *(grey squares)* and the reference (0%wt carbonate addition) cured for 1 day, 28 days and 90 days at 20 °C normalized to the clinker content.

896

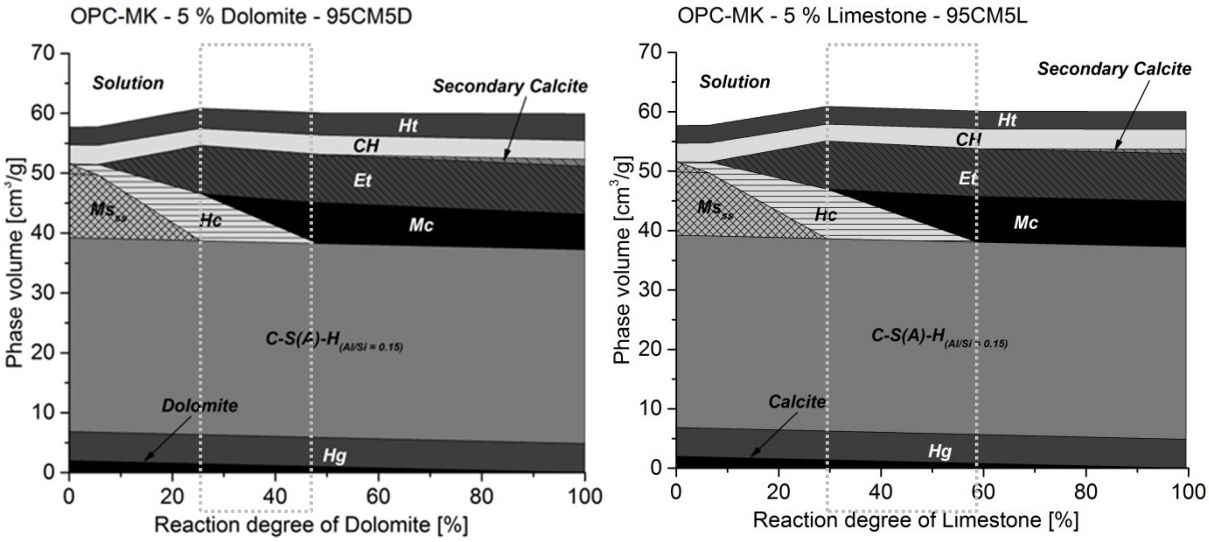

Figure 11: Effect of the degree of reaction of dolomite or limestone on the phase assemblage of a hydrated Portland metakaolin cement containing 5%wt of one of the carbonate sources. A composition of Portland cement clinker and metakaolin (Table 1) in the ratio 6:1 was used as input for the modelling. The modelled phases dolomite, hydrogrossular (Hg), C-S-(A)-H phase, monosulphate (Ms), hemicarbonate (Hc), monocarbonate (Mc), ettringite (Et), portlandite (CH), hydrotalcite (Ht) and secondary calcite are indicated. The dotted rectangles represent the area of the observed phase assemblage in the 5%wt samples of either dolomite or limestone after 90 days when cured at 20 °C.

897